Probabilistic physical characteristics of phase transitions at highway bottlenecks: Incommensurability of three-phase and two-phase traffic-flow theories

Boris S. Kerner,[1] Sergey L. Klenov,[2] and Michael Schreckenberg[1]
[1]*Physik von Transport und Verkehr, Universität Duisburg-Essen, 47048 Duisburg, Germany*
[2]*Moscow Institute of Physics and Technology, Department of Physics, 141700 Dolgoprudny, Moscow Region, Russia*
(Received 17 March 2014; published 13 May 2014)

Physical features of induced phase transitions in a metastable free flow at an on-ramp bottleneck in three-phase and two-phase cellular automaton (CA) traffic-flow models have been revealed. It turns out that at given flow rates at the bottleneck, to induce a moving jam (F→J transition) in the metastable free flow through the application of a time-limited on-ramp inflow impulse, in both two-phase and three-phase CA models *the same critical amplitude* of the impulse is required. If a smaller impulse than this critical one is applied, neither F→J transition nor other phase transitions can occur in the two-phase CA model. We have found that in contrast with the two-phase CA model, in the three-phase CA model, if the same smaller impulse is applied, then a phase transition from free flow to synchronized flow (F→S transition) can be induced at the bottleneck. This explains why rather than the F→J transition, in the three-phase theory traffic breakdown at a highway bottleneck is governed by an F→S transition, as observed in real measured traffic data. None of two-phase traffic-flow theories incorporates an F→S transition in a metastable free flow at the bottleneck that is the main feature of the three-phase theory. On the one hand, this shows *the incommensurability* of three-phase and two-phase traffic-flow theories. On the other hand, this clarifies why none of the two-phase traffic-flow theories can explain the set of fundamental empirical features of traffic breakdown at highway bottlenecks.

DOI: 10.1103/PhysRevE.89.052807 PACS number(s): 89.40.−a, 47.54.−r, 64.60.Cn, 05.65.+b

I. INTRODUCTION

Since three-phase traffic theory was introduced and formulated [1,2] and until now, there has been a highly controversial discussion about the question of what traffic-flow theory can better describe the physics of traffic breakdown observed at highway bottlenecks in real measured traffic data [3–16]. "Traffic breakdown at a highway bottleneck" describes the phenomenon of the phase transition from an initial free flow to congested traffic at the bottleneck [14,15,17–29]. During the breakdown vehicle speed sharply decreases, whereas the flow rate can remain as large as in an initial free flow (see empirical results presented in figures of [14–16,30]).

The importance of understanding real traffic breakdown at highway bottlenecks is as follows: (i) The capacity of free flow is restricted by traffic breakdown. (ii) The reliability of control and optimization of traffic and transportation networks depends crucially on whether traffic control can prevent traffic breakdown or not. (iii) The efficiency of dynamic traffic assignment in traffic and transportation networks depends crucially on whether the assignment can reduce traffic congestion in a network or not. Therefore each traffic-flow model and theory that can be reliably used for control and optimization in traffic networks should explain the set of empirical features of traffic breakdown.

From a huge number of traffic breakdown observations in different countries (see, e.g., [14–29]), the following common set of fundamental empirical features of traffic breakdown at a highway bottleneck has been distinguished:

1. Traffic breakdown at a highway bottleneck is a local phase transition from free flow (F) to congested traffic whose downstream front is usually fixed at the bottleneck location (see, e.g., [17,20–28] and references there). Such congested traffic we call synchronized flow (S) [14,15] [Figs. 1(a) and 1(b)]. This means that traffic breakdown is an F→S transition.

2. At the same bottleneck, traffic breakdown can be either spontaneous or induced [Fig. 1(b)] [14–16].

3. The probability of traffic breakdown is an increasing flow rate function [23–28].

4. There is a well-known hysteresis phenomenon associated with traffic breakdown and a return transition to free flow (e.g., [17,20,21]).

In accordance with general features of metastable systems of natural science (see, e.g., [32]), empirical features 2–4 of traffic breakdown mean that free flow at a highway bottleneck is in a metastable state with respect to the F→S transition. Therefore traffic breakdown and the F→S transition occurring in a metastable free flow at a highway bottleneck are synonyms.

There were two generally accepted traffic-flow theories introduced in the 1950s–1960s:

(i) The Lighthill-Whitham-Richards (LWR) model [33,34]. In the classic LWR model there is no traffic-flow instability. It is assumed that complex traffic-flow phenomena are caused by large amplitude disturbances in traffic [3,33,35,36].

(ii) The General Motors (GM) car-following model by Herman *et al.* [37] and Gazis *et al.* [38,39] (see reviews [40]) explains traffic breakdown by a traffic-flow instability associated with *an overdeceleration effect* as follows: If a vehicle begins to decelerate unexpectedly, then due to a finite driver reaction time, the following vehicle starts deceleration with a delay. As a result, the speed of the following vehicle becomes lower than the speed of the preceding vehicle. If this overdeceleration effect is realized for all following drivers, the traffic-flow instability occurs, leading to a growing wave of *vehicle speed reduction* in traffic flow. With the use of very different mathematical approaches, the overdeceleration effect has been incorporated in a huge number of traffic-flow models that can be considered belonging to the GM model class. This is because (as found first in [41–43]) in all these very different traffic-flow models, the overdeceleration effect leads

 ©2014 American Physical Society

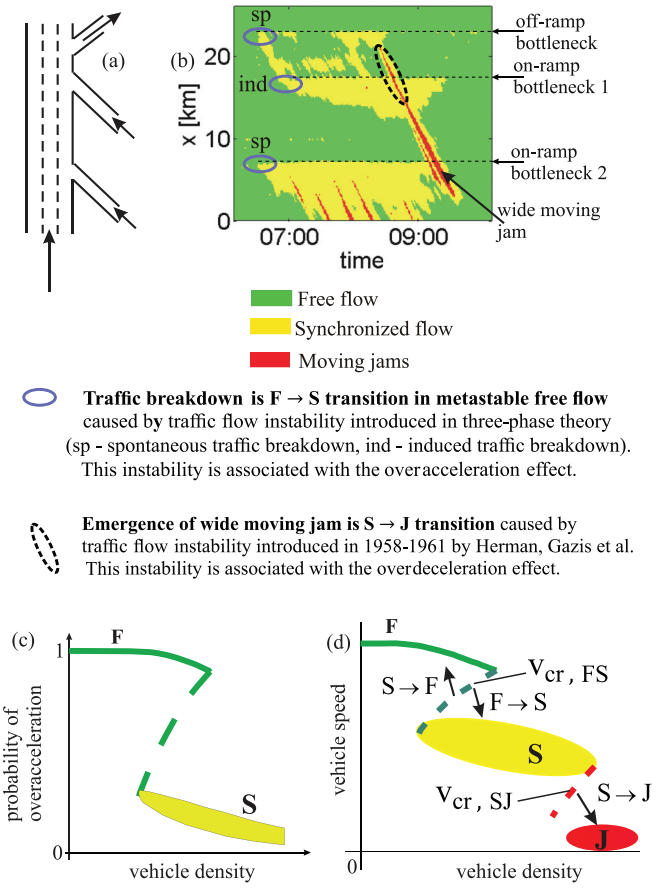

FIG. 1. (Color online) A known empirical example of phase transitions in traffic flow illustrating two traffic-flow instabilities of three-phase theory (real measured traffic data of road detectors installed along three-lane highway) [30]. (a) Sketch of section of three-lane highway in Germany with three bottlenecks. (b) Speed data measured with road detectors installed along road section in (a); data [14] are presented in space and time with averaging method described in Sec. C 2 of [31]. (c) Hypothesis of three-phase theory about discontinuous character of overacceleration probability [2,14,15]. (d) Hypothesis of three-phase theory about features of phase transitions in traffic flow: 2Z characteristic for phase transitions [14], F – free flow phase, S – synchronized flow phase, J – wide-moving jam phase. In (b), "sp" – spontaneous F→S transition, "ind" – induced F→S transition. In (d), $v_{cr,\,FS}$ is the branch for critical speed within local disturbance required for F→S or S→F transitions, labeled by associated arrows; $v_{cr,\,SJ}$ is the branch for critical speed within local disturbance required for S→J transition, labeled by associated arrow.

to a moving jam (J) formation in free flow (F) (F→J transition) (see references in [7,8,16,44]). The overdeceleration effect should explain a transition from free flow to congested traffic in traffic-flow models of the GM model class.

As explained in [14–16], the LWR theory [33–36] fails in the explanation of real traffic breakdown because the LWR theory cannot show induced traffic breakdown observed in real traffic. Two-phase traffic-flow models of the GM model class (see references in [14–17]) fail in the explanation of real traffic breakdown because rather than an F→S transition, traffic breakdown in the models of the GM class is an F→J transition.

The main reason for the three-phase theory is the explanation of traffic breakdown at a highway bottleneck rather than congestion resulting from the breakdown. In accordance with the fundamental empirical features of traffic breakdown at the bottleneck, in three-phase theory, traffic breakdown is an F→S transition in a metastable free flow.

To reach this goal, in the three-phase theory a traffic-flow instability has been introduced associated to *an overacceleration effect* as follows: It is assumed that due to a driver's time delay in overacceleration [45], between the free flow and synchronized flow phases, the probability of a driver's overacceleration from car-following exhibits a *discontinuous character* [2,14,15] [Fig. 1(c)]. This overacceleration effect leads to the instability that causes a growing wave of a local *increase* of the vehicle speed.

A competition of the overacceleration effect with the adaptation of the vehicle speed to the speed of the preceding vehicle should explain F→S and a return S→F transitions observed in real traffic [45]. In addition to the instability associated with the overacceleration effect, the three-phase theory incorporates the overdeceleration effect of the GM model class. In the three-phase theory, the overdeceleration effect explains moving jam emergence in synchronized flow (S→J transition) observed in real traffic [Fig. 1(b)].

Thus the characteristic feature of the three-phase theory is the assumption about the existence of two qualitatively different instabilities in vehicular traffic: (i) The instability associated with the overacceleration, causing a growing wave of vehicle speed *increase*. (ii) The instability of the GM model class associated with the overdeceleration effect that causes a growing wave of speed *reduction*. These two instabilities should explain complex phase transitions in vehicular traffic, as shown qualitatively on a 2Z characteristic of phase transitions of three-phase theory [Fig. 1(d)].

The first mathematical implementation of these hypotheses of three-phase theory [1,2,14,15] has been a stochastic continuous-in-space microscopic model [9], which has been further developed for different applications in [11,13,46]. Over time a number of other three-phase traffic-flow models have been developed (e.g., [31,47–96]) that incorporate some of the hypotheses of the three-phase theory.

However, both the two-phase theory associated with studies of the GM model class [7,8,44] and the three-phase theory [14,15] show a *metastable free flow* at a highway bottleneck. This free flow metastability leads to a complex dynamics of congested traffic patterns at highway bottlenecks found in both traffic-flow theories. This can explain the highly controversial discussion in the field of vehicular traffic physics mentioned above [4–16,44].

In this article, we try to resolve this highly controversial discussion based on the following methodology. We choose stochastic microscopic three-phase and two-phase traffic-flow models that incorporate the *same traffic-flow instability of the GM model class* leading to moving jam emergence. With the use of simulations of both models at the *same* model parameters, we analyze the critical disturbances required for induced phase transitions at the bottleneck.

To be sure that both three-phase and two-phase traffic-flow models exhibit the same *quantitative* characteristics of

moving jams, we choose the Kerner-Klenov-Schreckenberg-Wolf (KKSW) three-phase cellular automaton (CA) traffic-flow model of Ref. [48]. Then we remove those terms of the KKSW CA model that describe mathematically the overacceleration effect. We find that the three-phase KKSW CA model transforms into the Nagel-Schreckenberg (NaSch) CA model [97–99] that belongs to the GM model class. By the transformation from the KKSW CA model into the NaSch CA model, no changes in model terms and parameters responsible for moving jam characteristics are made. We find that this procedure does result in the same quantitative characteristics of moving jams in both CA models.

In comparison with previous studies of three-phase traffic theory [10,14–16,48,89] and the NaSch CA model [97–99], we focus on an analysis of features of *induced* phase transitions at an on-ramp bottleneck in the KKSW and NaSch CA models. We have found that at given flow rates at the bottleneck, to induce an F→J transition in a metastable free flow at the bottleneck through the application of a time-limited on-ramp inflow impulse, in both the KKSW and NaSch CA models *the same critical amplitude* of the impulse is required. If a smaller on-ramp inflow impulse than this critical one is applied, neither F→J transition nor other phase transitions can occur in the NaSch CA model: Free flow recovers at the bottleneck. In contrast with the NaSch CA model, in the KKSW CA model, if the same smaller impulse is applied, then an F→S transition can be induced at the bottleneck. This explains why rather than the F→J transition, in the three-phase theory traffic breakdown at a highway bottleneck is governed by the F→S transition, as observed in real measured traffic data. None of the two-phase traffic-flow theories incorporates an F→S transition in a metastable free flow at the bottleneck, which is the main feature of the three-phase theory. This shows the incommensurability of three-phase and two-phase traffic-flow theories.

The article is organized as follows. Features of induced traffic breakdown at an on-ramp bottleneck in the KKSW CA model is the subject of Sec. II. In Sec. III, we analyze the probability of phase transitions in a metastable free flow at the bottleneck in the NaSch CA model. In Sec. IV we discuss the basic difference of probabilistic features of phase transitions in three-phase and two-phase traffic-flow theories. In the Discussion section (Sec. V), we make a comparison of threshold and critical characteristics of phase transitions in three-phase and two-phase theories (Sec. V A), and make an explanation of macroscopic and microscopic definitions of synchronized flow and wide-moving jam phases (Sec. V B), as well as formulate conclusions.

II. INDUCED TRAFFIC BREAKDOWN AT ON-RAMP BOTTLENECK IN KKSW CA MODEL

A. KKSW CA model

In the KKSW CA model for a single-lane road for identical vehicles [48], the following designations for main variables and vehicle parameters are used: $n = 0,1,2,\ldots$ is the number of time steps; $\tau = 1$ s is time step; $\delta x = 1.5$ m is space step; x_n and v_n are the coordinate and speed of the vehicle; time and space are measured in units of τ and δx, respectively;

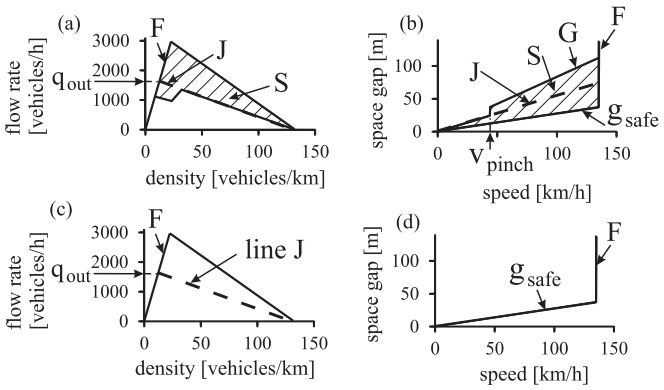

FIG. 2. Steady states of the KKSW CA model (a, b) and NaSch CA model (c, d) in the flow-density (a, c) and space-gap–speed planes (b, d). G and g_{safe} are, respectively, a synchronization gap and a safe gap at a time-independent speed v (where $g_{safe} = v$), F – free flow, S – synchronized flow [hatched 2D regions in (a, b)], J – line J. In (a,c), line J represents the downstream front of a wide-moving jam in the flow-density plane, q_{out} is the flow rate in free flow related to the outflow from the wide-moving jam. In (b), the model parameter v_{pinch} is explained after formula (16).

v_{free} is the maximum speed in free flow; the lower index ℓ marks variables related to the preceding vehicle; d is vehicle length; $g_n = x_{\ell,n} - x_n - d$ is a space gap between two vehicles following each other; and G_n is a synchronization space gap [Figs. 2(a) and 2(b)].

The KKSW CA model consists of the following sequence of rules:

(a) "Comparison of vehicle gap with the synchronization gap:"

$$\text{if } g_n \leqslant G(v_n)$$
$$\text{then follow rules (b) and (c), and skip rule (d),} \quad (1)$$

$$\text{if } g_n > G(v_n)$$
$$\text{then skip rules (b) and (c), and follow rule (d).} \quad (2)$$

(b) "Speed adaptation within synchronization gap" is given by the formula

$$v_{n+1} = v_n + \text{sgn}(v_{\ell,n} - v_n). \quad (3)$$

(c) "Overacceleration through random acceleration within a synchronization gap" is given by the formula

$$\text{if } v_n \geqslant v_{\ell,n}, \text{ then with probability } p_a,$$
$$v_{n+1} = \min(v_{n+1} + 1,\ v_{free}). \quad (4)$$

(d) "Acceleration:"

$$v_{n+1} = \min(v_n + 1,\ v_{free}). \quad (5)$$

(e) "Deceleration:"

$$v_{n+1} = \min(v_{n+1},\ g_n). \quad (6)$$

(f) "Randomization" is given by the formula

$$\text{with probability } p, \quad v_{n+1} = \max(v_{n+1} - 1,\ 0). \quad (7)$$

(g) "Motion" is described by the formula

$$x_{n+1} = x_n + v_{n+1}. \tag{8}$$

Formula (4) is applied when

$$r < p_a, \tag{9}$$

and formula (7) is applied when

$$p_a \leqslant r < p_a + p, \tag{10}$$

where $p_a + p \leqslant 1$; $r = rand()$ is a random value distributed uniformly between 0 and 1. Probability of overacceleration p_a in (4) is chosen as the increasing speed function:

$$p_a(v_n) = p_{a,1} + p_{a,2} \max[0, \min(1, (v_n - v_{syn})/\Delta v_{syn})], \tag{11}$$

where $p_{a,1}$, $p_{a,2}$, v_{syn}, and Δv_{syn} are constants. In (1)–(11),

$$G(v_n) = k v_n. \tag{12}$$

The rules of vehicle motion (2)–(12) [without formula (11)] have been formulated in the KKW CA model [10]. In comparison with the KKW CA model, we use in (7), (10) for probability p the formula

$$p = \begin{cases} p_2 & \text{for} \quad v_{n+1} > v_n, \\ p_3 & \text{for} \quad v_{n+1} \leqslant v_n, \end{cases} \tag{13}$$

which has been used in the KKSW CA model of Ref. [48]. The importance of formula (13) is as follows. This rule of vehicle motion leads to a time delay in vehicle acceleration at the downstream front of synchronized flow. In other words, this is an additional mechanism of time delay in vehicle acceleration in comparison with the slow-to-start rule of the NaSch CA model [98],

$$p_2(v_n) = \begin{cases} p_0^{(2)} & \text{for} \quad v_n = 0, \\ p_1^{(2)} & \text{for} \quad v_n > 0, \end{cases} \tag{14}$$

that is also used in the KKSW CA model. However, in the KKSW CA model in formula (14), probability $p_1^{(2)}$ is chosen to provide a delay in vehicle acceleration only if the vehicle does not accelerate at the previous time step n:

$$p_1^{(2)} = \begin{cases} p_2^{(2)} & \text{for} \quad v_n \leqslant v_{n-1}, \\ 0 & \text{for} \quad v_n > v_{n-1}. \end{cases} \tag{15}$$

In (13)–(15), p_3, $p_0^{(2)}$, and $p_2^{(2)}$ are constants.

To describe the pinch effect resulting in spontaneous wide-moving jam emergence in synchronized flow (S→J transition) [14], we also assume that in (12) [10],

$$k(v_n) = \begin{cases} k_1 & \text{for} \quad v_n > v_{pinch}, \\ k_2 & \text{for} \quad v_n \leqslant v_{pinch}, \end{cases} \tag{16}$$

where v_{pinch}, k_1, and k_2 are constants ($k_1 > k_2 \geqslant 1$). The model parameter v_{pinch} defines a range of speeds in synchronized flow $0 < v \leqslant v_{pinch}$ [Fig. 2(b)] within which wide-moving jams occur spontaneously with a larger probability.

The rule of vehicle motion (13) of the KKSW CA model [48] together with formula (11) allows us to improve the characteristics of synchronized flow patterns (SP) simulated with such a new version of the KKSW CA model (2)–(16) for a single-lane road. Other physical features of the KKSW CA model have been explained in [48]. A model of an on-ramp bottleneck is the same as that presented in [89]. Parameters of the KKSW CA model used in simulations are presented in Table I. Open road boundary conditions are used; the boundary and initial conditions are the same as those used in the KKS CA model [89].

TABLE I. Model parameters of the KKSW and NaSch CA models used in simulations.

Parameters for vehicle motion in road lane:
$d = 5$ (7.5 m), $v_{free} = 25$ (135 km/h),
$p_3 = 0.01$, $p_0^{(2)} = 0.5$,
$v_{pinch} = 8$ (43.2 km/h), $k_1 = 3$, $k_2 = 2$.
$p_{a,1} = 0.07$, $p_{a,2} = 0.08$, $p_2^{(2)} = 0.35$,
$v_{syn} = 14$ (75.6 km/h), $\Delta v_{syn} = 3$ (16.2 km/h)

Because a competition between speed adaptation and overacceleration determines F→S and S→F transitions (Sec. I), it is useful to discuss the description of these effects with the KKSW CA model. In the KKSW CA model, the speed adaptation effect in synchronized flow of three-phase theory [14] takes place within the space gap range [Fig. 2(b)]

$$g_{safe,\,n} \leqslant g_n \leqslant G_n, \tag{17}$$

where $g_{safe,\,n}$ is a safe space gap, $g_{safe,\,n} = v_n$. Under condition (17), formula (3) is valid, i.e., the vehicle tends to adjust its speed to the preceding vehicle without caring what the precise space gap is, as long as it is safe. The vehicle accelerates or decelerates in dependence on whether the vehicle moves slower or faster than the preceding vehicle, respectively. In other words, there is both "negative" and "positive" velocity adaptation.

In the KKSW CA model, the overacceleration is simulated as a collective effect that occurs on average in traffic flow through the use of random vehicle acceleration given by formula (4). Probability of overacceleration p_a in (4) is responsible for the existence of a time delay in the overacceleration; the time delay [45] is required in the three-phase theory to simulate the discontinuous character of the overacceleration between metastable states of free flow and synchronized flow [Fig. 1(c)]. The overacceleration (4) occurs only under conditions (17) and

$$v_n \geqslant v_{\ell,n}. \tag{18}$$

In accordance with the three-phase theory [15], under condition (17) overacceleration takes place even if the vehicle is not currently slower than the preceding vehicle and the preceding vehicle does not accelerate.

Thus in the KKSW CA model the description of the overacceleration and overdeceleration are related to the S→F and F→J phase transitions, respectively. It must be stressed that this is true also for many other three-phase traffic-flow models. In particular, as explained in detail in Sec. 16.3 of [14], very similar descriptions of overacceleration and overdeceleration have been used in the continuous-space models of Ref. [9,11].

B. Characteristics of induced traffic breakdown (induced F→S transition)

In the KKSW CA model (1)–(16), free flow at the bottleneck is in a metastable state with respect to an F→S transition (traffic breakdown) within the flow rate range between a minimum capacity $C_{\min}$ and a maximum capacity $C_{\max}$ of free flow at the bottleneck:

$$C_{\min} \leqslant q_{\text{sum}} < C_{\max}, \tag{19}$$

where

$$q_{\text{sum}} = q_{\text{in}} + q_{\text{on}} \tag{20}$$

is the flow rate downstream of the bottleneck, q_{in} is the flow rate on the main single-lane road upstream of the bottleneck, and q_{on} is the on-ramp inflow rate. Under condition (19), the F→S transition can be induced through the application of a time-limited disturbance in free flow at the bottleneck whose amplitude exceeds some critical value [100]. To simulate such a critical disturbance in free flow at the bottleneck, we have used an on-ramp inflow impulse applied during a time interval Δt_{ind}. When the amplitude of this impulse reaches a critical value denoted by Δq_{on}, an F→S transition occurs at the bottleneck (Fig. 3). During the time interval Δt_{ind}, the resulting on-ramp inflow is equal to $q_{\text{on}} + \Delta q_{\text{on}}$.

The critical amplitude of the impulse of on-ramp inflow rate $\Delta q_{\text{on}}(q_{\text{sum}})$ is a decreasing function of the flow rate downstream of the bottleneck q_{sum} [Fig. 3(a)]. Moreover, the longer the disturbance duration Δt_{ind}, the smaller the critical amplitude of the impulse Δq_{on} is required to induce the breakdown [curves 1 and 2 in Fig. 3(a)] [101]. Within the flow rate range (19) there are two qualitative different flow rate ranges within which induced traffic breakdown at the bottleneck exhibits different statistical features.

Within the flow rate range

$$q_{\text{th}}^{(\text{B})} \leqslant q_{\text{sum}} < C_{\max}, \tag{21}$$

both spontaneous and induced traffic breakdowns are possible. A random time-delayed spontaneous traffic breakdown occurs during the time interval T_{ob} [Figs. 4(a) and 4(b)] with the probability $0 < P^{(\text{B})}(q_{\text{sum}}) < 1$ [102]. Here $q_{\text{th}}^{(\text{B})}$ is a threshold flow rate for spontaneous traffic breakdown. However, because under conditions (21) the breakdown probability $0 < P^{(\text{B})}(q_{\text{sum}}) < 1$, in some of the simulation realizations no breakdown occurs during the time interval T_{ob} [realization 3

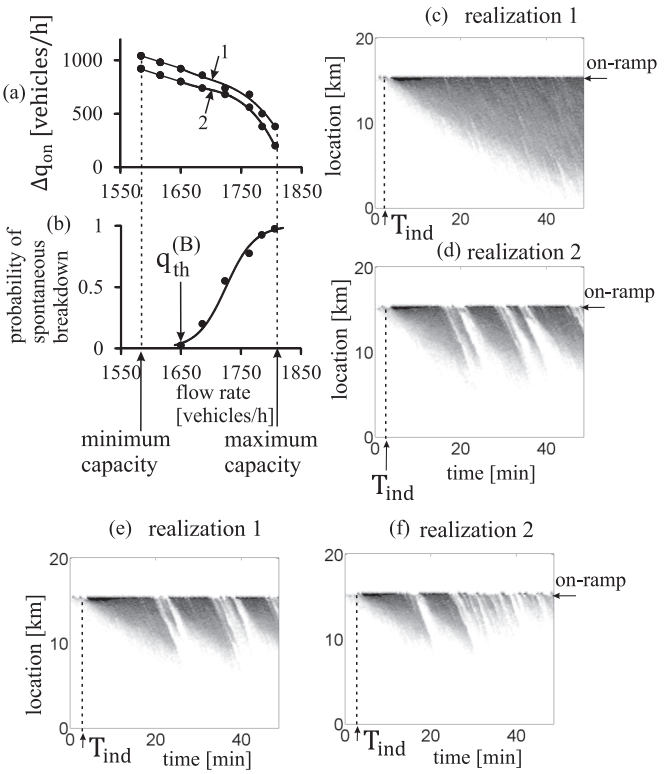

FIG. 3. Induced traffic breakdown in KKSW CA model (1)–(16). (a) Dependence of critical impulse amplitude $\Delta q_{\text{on}}(q_{\text{sum}})$ on the flow rate q_{sum} downstream of the bottleneck. (b) Dependence of the probability of spontaneous traffic breakdown $P^{(\text{B})}(q_{\text{sum}})$ on the flow rate q_{sum} calculated at $T_{\text{ob}} = 30$ min and $N = 40$ [102]. (Breakdown probability in (b) is qualitatively the same as found earlier in [48].) In (a), the impulse of on-ramp inflow rate Δq_{on} with a duration $\Delta t_{\text{ind}} = 1$ min (curve 1) and 2 min (curve 2) is applied beginning at $T_{\text{ind}} = 3$ min. (c–f) Different simulation realizations for synchronized flow patterns (SP) resulting from induced breakdown at the on-ramp bottleneck for $(q_{\text{in}}, \Delta q_{\text{on}}) = (1216, 920)$ (c, d) and (1185, 980) vehicles/h (e, f); $\Delta t_{\text{ind}} = 1$ min; speed data presented by regions with variable shades of gray (in white regions the speed is equal to or higher than 120 km/h, in black regions the speed is zero); $q_{\text{on}} = 400$ vehicles/h. Calculated minimum capacity $C_{\min} = 1585$ vehicles/h. Calculated maximum capacity $C_{\max} = 1810$ vehicles/h. Location of the on-ramp bottleneck is $x_{\text{on}} = 15$ km.

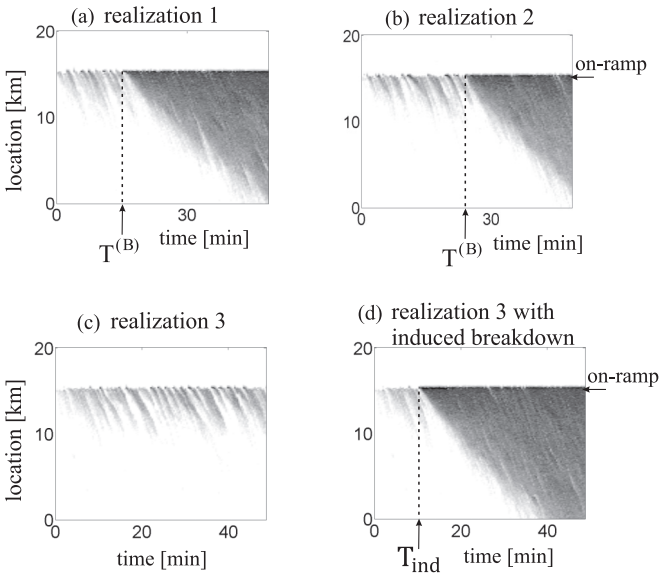

FIG. 4. Induced breakdown in KKSW CA model under conditions (21). Speed data presented by regions with variable shades of gray (in white regions the speed is equal to or higher than 120 km/h, in black regions the speed is zero). Three different simulation realizations 1–3 in (a–c) are related to $P_{\text{FS}}^{(\text{B})} = 0.775$ calculated at $q_{\text{in}} = 1364$ vehicles/h and $q_{\text{on}} = 400$ vehicles/h. In (d), traffic breakdown has been induced in realization 3 (c) due to the impulse of on-ramp inflow $\Delta q_{\text{on}} = 680$ vehicles/h of duration $\Delta t_{\text{ind}} = 1$ min that is applied at $t = T_{\text{ind}} = 10$ min. Other parameters are the same as those in Fig. 3.

in Fig. 4(c)]. However, traffic breakdown can be induced in this simulation realization [Fig. 4(d)]. We have found that independent of whether spontaneous or induced breakdown has occurred, in the KKSW CA model traffic breakdown is an F→S transition [Figs. 3(c)–3(f) and 4(d)], as observed in empirical traffic data [14,15,103].

Within the flow rate range

$$C_{\min} \leqslant q_{\text{sum}} < q_{\text{th}}^{(\text{B})}, \tag{22}$$

only induced traffic breakdown is possible at the bottleneck. This is because under condition

$$q_{\text{sum}} < q_{\text{th}}^{(\text{B})} \tag{23}$$

the probability of spontaneous breakdown at the bottleneck is $P^{(\text{B})}(q_{\text{sum}}) = 0$ [Fig. 3(b)].

III. PROBABILISTIC FEATURES OF TRAFFIC FLOW INSTABILITY IN FREE FLOW AT ON-RAMP BOTTLENECK IN THE NAGEL-SCHRECKENBERG CA MODEL

A. Derivation of NaSch CA model from KKSW CA model

To derive a two-phase traffic-flow model from the KKSW CA model, we remove in the KKSW CA model the following terms, which incorporate hypotheses of three-phase theory: (i) 2D region of steady states for synchronized flow described by Eqs. (1), (12), and (16); as a result, steady states of a new CA model lie on the fundamental diagram [Figs. 2(c) and 2(d)]. (ii) "Speed adaptation within a synchronization gap" described by Eq. (3). (iii) "Overacceleration through random acceleration within the synchronization gap," described by Eqs. (4), (9), and (11). The remaining model rules of vehicle motion are as follows:

(a) "Acceleration:"

$$v_{n+1} = \min(v_n + 1,\ v_{\text{free}}); \tag{24}$$

(b) "Deceleration:"

$$v_{n+1} = \min(v_{n+1},\ g_n); \tag{25}$$

(c) "Randomization" is given by the formula

$$\text{with probability } p, \quad v_{n+1} = \max(v_{n+1} - 1,\ 0); \tag{26}$$

(d) "Motion" is described by the formula

$$x_{n+1} = x_n + v_{n+1}. \tag{27}$$

In (26), we use for probability p formulas (13), (14), and (15). We see that the resulting two-phase CA model is the NaSch CA model with the slow-to-start rule [97].

B. Probability of spontaneous F→J transition at on-ramp bottleneck in NaSch CA model

In accordance with well-known results [44,97], in the NaSch CA model (24)–(27), (13)–(15) spontaneous instability of free flow at the bottleneck leads to an F→J transition in metastable free flow at the bottleneck (Fig. 5). As a result of the F→J transition, wide-moving jams emerge in the NaSch CA model [Figs. 5(b) and 5(c)]. We also come to another well-known result [7,8,44,97] found first from a study of a deterministic model of the GM model class [42,43] that within the flow rate range

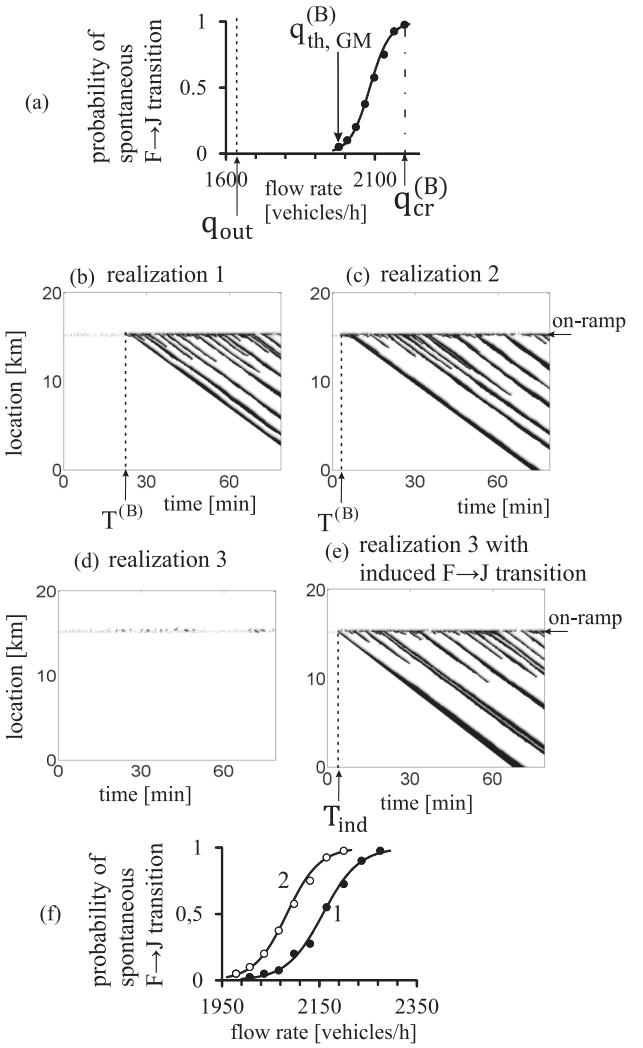

FIG. 5. Probabilistic features of F→J transition in the NaSch CA model (24)–(27). (a) Dependence of probability of spontaneous F→J transition $P_{\text{GM}}^{(\text{B})}(q_{\text{sum}})$ on the flow rate q_{sum} at given values of on-ramp inflow rate $q_{\text{on}} = 400$ vehicles/h, time interval $T_{\text{ob}} = 30$ min, and value $N = 40$ [q_{on}, T_{ob}, and N are, respectively, the same as those in the study of the breakdown probability in KKSW CA model shown in Fig. 3(b)]. (b–e) Speed data presented by regions with variable shades of gray (in white regions the speed is equal to or higher than 120 km/h, in black regions the speed is zero). In (b–d), three different simulation realizations 1–3 related to $P_{\text{GM}}^{(\text{B})} = 0.775$ calculated at $q_{\text{in}} = 1731$ vehicles/h are shown. In (e), F→J transition has been induced in realization 3 (d) due to the impulse of on-ramp inflow $\Delta q_{\text{on}} = 200$ vehicles/h of duration $\Delta t_{\text{ind}} = 1$ min that is applied at $T_{\text{ind}} = 3$ min (marked by vertical dashed lines). (f) Comparison of probability of F→J transition for $T_{\text{ob}} = 10$ (curve 1) and 30 min [curve 2 is taken from (a)]. Calculated flow rates marked in (a) are $q_{\text{out}} = 1636$, $q_{\text{th, GM}}^{(\text{B})} = 1979$, $q_{\text{cr}}^{(\text{B})} = 2220$ vehicles/h. Other parameters are the same as those in Fig. 4.

$$q_{\text{out}} \leqslant q_{\text{sum}} < q_{\text{cr}}^{(\text{B})}, \tag{28}$$

free flow is in a metastable state with respect to the F→J transition. In (28), q_{out} is the characteristic flow rate related to

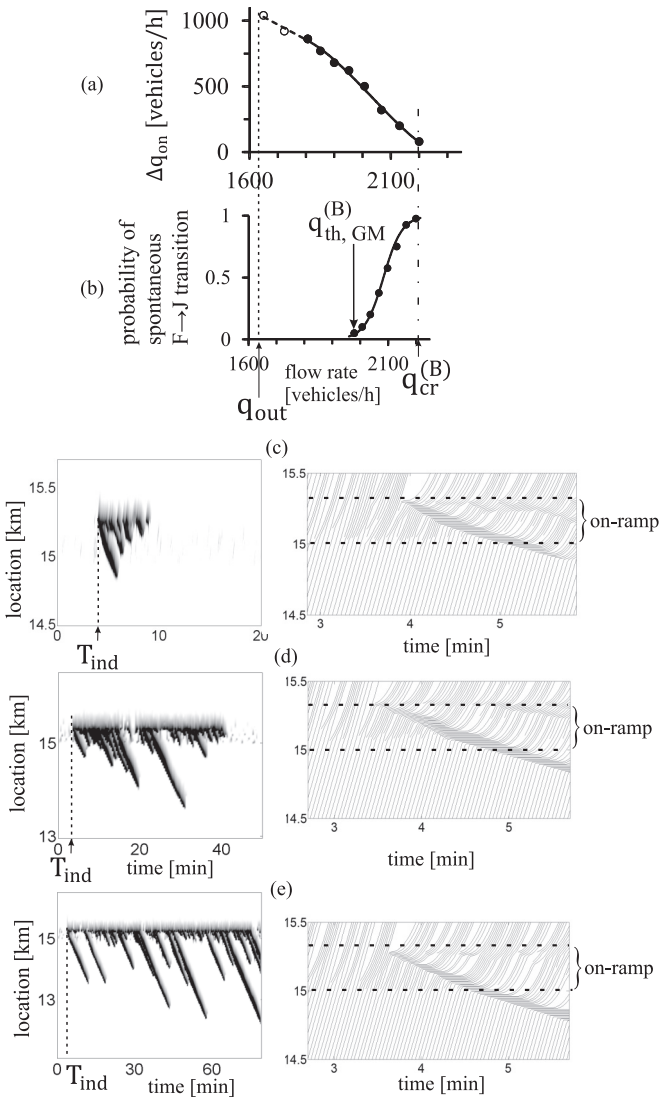

FIG. 6. Induced F→J transition in NaSch CA model (24)–(27). (a) Dependence of the critical impulse of on-ramp inflow Δq_{on} on the flow rate downstream of the on-ramp bottleneck q_{sum} at $q_{on} =$ 400 vehicles/h. (b) Probability of spontaneous F→J transition taken from Fig. 5(a). (c–e) Induced F→J transition under condition (31) at $(q_{in},\ \Delta q_{on}) = (1250, 1040)$ (c), (1324, 920) (d), and (1406, 860) (e) vehicles/h; $q_{on} = 400$ vehicles/h. In (c–e), left panel – speed data presented by regions with variable shades of gray (in white regions the speed is equal to or higher than 120 km/h, in black regions the speed is zero); right panel – vehicle trajectories. Impulse Δq_{on} of duration $\Delta t_{ind} = 1$ min is applied at $T_{ind} = 3$ min. Other parameters are the same as those in Fig. 5.

free flow in the wide-moving jam outflow [Fig. 2(c)], and $q_{cr}^{(B)}$ is a critical flow rate at which the instability of the GM model class occurs at the bottleneck.

We have also found the following results (Figs. 5 and 6). There is a flow rate range

$$q_{th,\ GM}^{(B)} \leqslant q_{sum} < q_{cr}^{(B)} \tag{29}$$

within which the probability $P_{GM}^{(B)}(q_{sum})$ of the occurrence of spontaneous F→J transition during a time interval T_{ob} satisfies conditions $0 < P_{GM}^{(B)}(q_{sum}) < 1$; the probability $P_{GM}^{(B)}(q_{sum})$ is an increasing flow rate function [Fig. 5(a)]. The probability $P_{GM}^{(B)}(q_{sum})$ is related to the occurrence of the F→J transition at the bottleneck during a given time interval T_{ob} in n of N simulation realizations (runs): $P_{GM}^{(B)}(q_{sum}) = n/N$, where N is number of realizations used for probability calculations. In this probabilistic analysis, the critical flow rate $q_{sum} = q_{cr}^{(B)}$ in (28) and (29) is related to the probability $P_{GM}^{(B)}(q_{cr}^{(B)}) = 1$.

In (29), $q_{sum} = q_{th,\ GM}^{(B)}$ is a threshold flow rate for the F→J transition. Under condition

$$q_{sum} < q_{th,\ GM}^{(B)}, \tag{30}$$

the probability of spontaneous F→J transition at the bottleneck is $P_{GM}^{(B)}(q_{sum}) = 0$.

C. Induced F→J transition at on-ramp bottleneck in NaSch CA model

We have also found that although under conditions

$$q_{out} \leqslant q_{sum} < q_{th,\ GM}^{(B)} \tag{31}$$

the probability of spontaneous F→J transition at the bottleneck is $P_{GM}^{(B)}(q_{sum}) = 0$, an F→J transition can be induced at the bottleneck. An induced F→J transition is possible in the whole flow rate range (28), within which free flow is in a metastable state with respect to the F→J transition. The critical amplitude $\Delta q_{on}(q_{sum})$ of the on-ramp inflow impulse that induces the F→J transition is a decreasing flow rate function [Fig. 6(a)].

There is a value of the flow rate $q_{sum} = q_{sum}^{(jam)}$ that satisfies conditions $q_{out} < q_{sum}^{(jam)} < q_{th,\ GM}^{(B)}$. At $q_{out} \leqslant q_{sum} < q_{sum}^{(jam)}$ [dashed part of the curve in Fig. 6(a)], a moving jam(s) that has been induced at the bottleneck dissolves during some time interval [Figs. 6(c) and 6(d)]; as a result, free flow recovers at the bottleneck. The smaller the difference $q_{sum} - q_{out}$, the shorter the time interval of jam dissolution.

IV. BASIC DIFFERENCE OF PROBABILISTIC FEATURES OF PHASE TRANSITIONS IN THREE-PHASE AND TWO-PHASE TRAFFIC FLOW THEORIES

In accordance with well-known results [4–15], in our probabilistic analysis of stochastic three-phase and two-phase traffic-flow models (Secs. II and III), we have confirmed that both the three-phase theory and the two-phase theory exhibit ranges of the flow rate q_{sum} downstream of a highway bottleneck within which free flow is in a metastable state. This means that a transition from this free flow to congested traffic can either occur spontaneously or be induced at the bottleneck. Therefore a question arises: What is the basic difference between the three-phase and two-phase theories?

To answer this question, first we discuss an important *common feature* of these theories. As in the NaSch CA model (Sec. III), in the KKSW CA model an F→J transition can be induced at the bottleneck (Fig. 7). This is because the both models incorporate the same overdeceleration effect of the GM model class.

Moreover, in the KKSW and NaSch CA models there is the same mean time delay from vehicle acceleration at the downstream front of a wide-moving jam $\tau_{del,\ J}^{(acc)}$ given by the

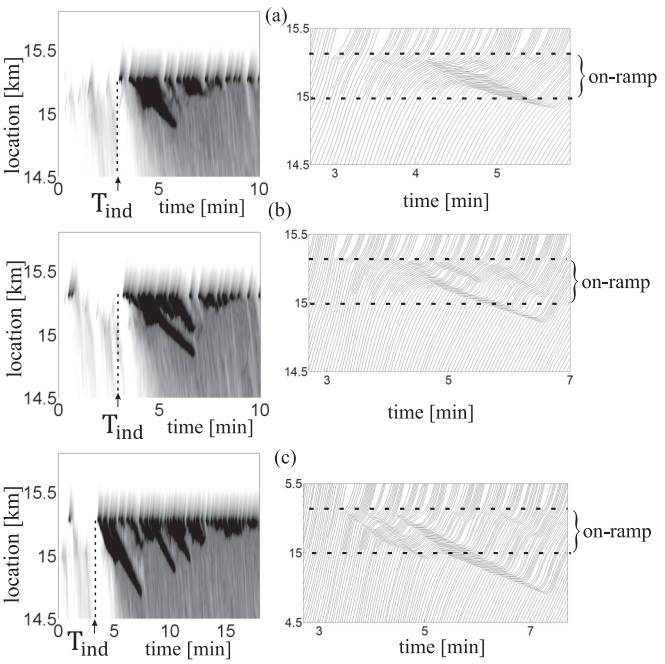

FIG. 7. Induced F→J transition in KKSW CA model (1)–(16) at the same values of on-ramp inflow rate $q_{on} = 400$ vehicles/h and the same critical amplitude of impulse of on-ramp inflow Δq_{on} as those values, respectively, used in Figs. 6(c)–6(e) for the NaSch CA model. Left panel – speed data presented by regions with variable shades of gray (in white regions the speed is equal to or higher than 120 km/h, in black regions the speed is zero), right panel – vehicle trajectories. As in Fig. 6, $(q_{in},\ \Delta q_{on}) = (1250, 1040)$ (a), (1324, 920) (b), and (1406, 860) (c) vehicles/h. Impulse Δq_{on} of duration $\Delta t_{ind} = 1$ min is applied at $T_{ind} = 3$ min. Other parameters are the same as those in Fig. 3.

well-known formula [97]

$$\tau_{del,\,J}^{(acc)} = \frac{\tau}{1 - p_0^{(2)}}, \tag{32}$$

where, in accordance with (14), $1 - p_0^{(2)}$ is the probability for vehicle acceleration from a standstill within the jam (for model parameters used in the KKSW and NaSch CA models, $\tau_{del,\,J}^{(acc)} = 2$ s). This leads to the same threshold flow rate q_{out} for the F→J transition:

$$q_{out} = \frac{3600}{\tau_{del,\,J}^{(acc)} + d/v_{free}}\,[\text{vehicles/h}]. \tag{33}$$

We have found that under conditions

$$q_{out} \leqslant q_{sum} < C_{max}, \tag{34}$$

an F→J transition of the GM model class can indeed be induced in the KKSW CA model (Fig. 7). A limitation for the flow rate q_{sum} associated with conditions (34) is caused by a spontaneous F→S transition that occurs in the KKSW CA model with the probability $P^{(B)} = 1$ at $q_{sum} \geqslant C_{max}$.

We have found the following results:

(i) At any flow rate q_{sum} (34) at which induced F→J transition in the KKSW CA model is possible (Fig. 7), the critical disturbance $\Delta q_{on}(q_{sum})$ required for induced F→J transition in the KKSW CA model coincides with that required for induced F→J transition in the NaSch found in Sec. III C (Fig. 8, curve 1). This result shows that both the three-phase and two-phase theories under conditions (34) exhibit the same features of induced F→J transition at highway bottlenecks.

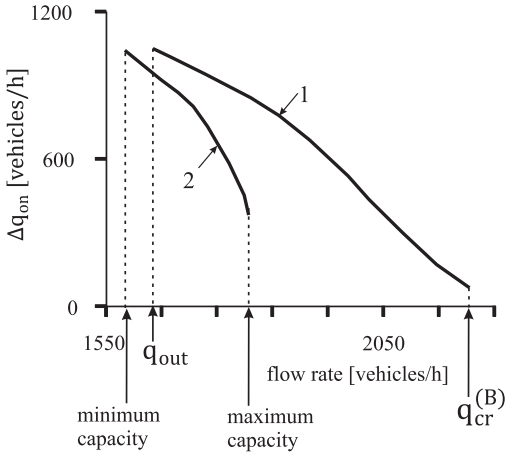

FIG. 8. Comparison of flow-rate dependencies of critical disturbances $\Delta q_{on}(q_{sum})$ that are required for induced F→J transition in the KKSW and NaSch CA models (curve 1) and that are required for induced F→S transition in the KKSW CA model (curve 2). Curves 1 and 2 are taken from Figs. 6(a) and 3(a), respectively. $\Delta t_{ind} = 1$ min.

(ii) In the KKSW CA model, under conditions (34) at any given flow rate q_{sum} the critical amplitude $\Delta q_{on} = \Delta q_{on}^{(FJ)}$ required for induced F→J transition (curve 1 in Fig. 8) is considerably *larger* than the critical amplitude $\Delta q_{on} = \Delta q_{on}^{(FS)}$ required for induced F→S transition (curve 2 in Fig. 8):

$$\Delta q_{on}^{(FJ)}(q_{sum}) > \Delta q_{on}^{(FS)}(q_{sum}). \tag{35}$$

Therefore synchronized flow patterns (SPs) occur at the bottleneck (Fig. 9) under application of considerably smaller disturbances in free flow at the bottleneck than disturbances required for the occurrence of moving jams (Fig. 7). In other words, in the three-phase theory the probability of F→S transition at the bottleneck is considerably larger than the probability of F→J transition.

V. DISCUSSION

A. Threshold and critical characteristics of phase transitions in three-phase and two-phase traffic-flow theories

The basic difference between the three-phase and two-phase traffic theories discussed above (Sec. IV) becomes more obvious when we compare the physical sense of the minimum highway capacity C_{min} and threshold flow rate q_{out}.

In both the three-phase and two-phase theories, the characteristic flow rate q_{out} is the minimum flow rate q_{sum} downstream of the bottleneck [Fig. 10(a)] at which an F→J transition is still possible to induce (Sec. IV).

In contrast, C_{min} is the minimum flow rate q_{sum} downstream of the bottleneck [Fig. 10(b)] at which an F→S transition, i.e., traffic breakdown is still possible to induce.

In contrast with the KKSW CA model, in the NaSch CA model no F→S transition is possible. Therefore the minimum highway capacity C_{min} of the three-phase theory has no sense for the two-phase traffic theory. This emphasizes

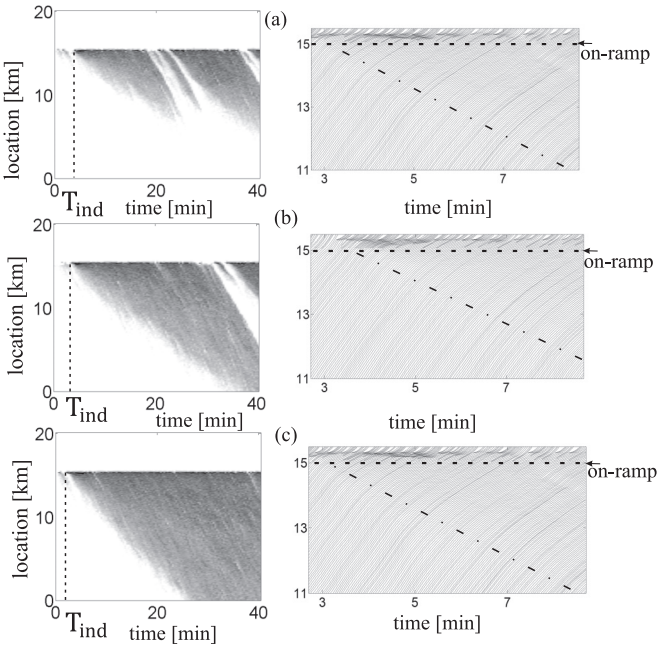

FIG. 9. Induced F→S transition in KKSW CA model (1)–(16) simulated at the same flow rates q_{on} and q_{in}, respectively, as those flow rates used in Fig. 7, however, at smaller values of critical amplitude of on-ramp inflow impulse Δq_{on}. Left panel – speed data presented by regions with variable shades of gray (in white regions the speed is equal to or higher than 120 km/h, in black regions the speed is zero); right panel – vehicle trajectories. $(q_{in}, \Delta q_{on}) =$ (1250, 920) (a), (1324, 740) (b), and (1406, 380) (c) vehicles/h, $q_{on} = 400$ vehicles/h. Dashed-dotted lines (right panel) mark the propagation of the upstream fronts of associated WSPs (left panel). Impulse Δq_{on} of duration $\Delta t_{ind} = 1$ min is applied at $T_{ind} = 3$ min. Other parameters are the same as those in Fig. 3.

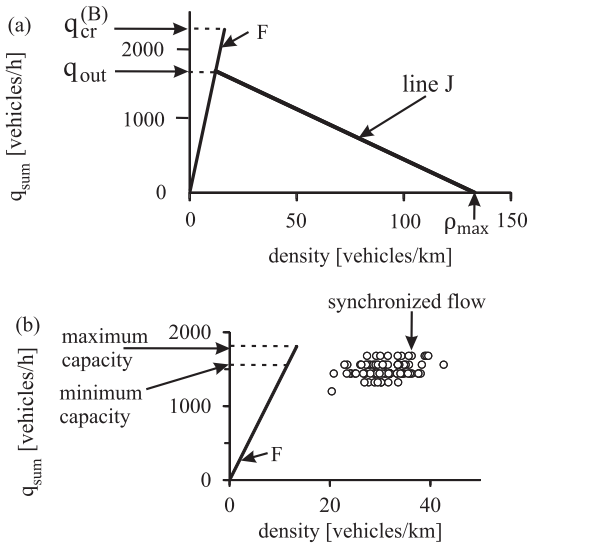

FIG. 10. Threshold and critical flow rates at the bottleneck in three-phase and two-phase traffic-flow theories. Metastable free flow in the GM motor class (a) and in three-phase theory (b) in the flow-density plane. Synchronized flow (1 min averaged data measured at location 15.32 km) is related to WSP shown in Fig. 4(a). In (a), $\rho_{max} = 1000/d$ is the vehicle density within a wide-moving jam.

the fundamental physical difference between threshold values C_{min} and q_{out}.

At model parameters chosen in Fig. 8, the condition

$$C_{min} < q_{out} \tag{36}$$

is satisfied. In the case

$$C_{min} \leqslant q_{sum} < q_{out}, \tag{37}$$

no F→J transition is possible. Therefore, under condition (37), only the F→S transition can occur at the bottleneck in the KKSW CA model. In contrast, in the NaSch CA model at any flow rate $q_{sum} < q_{out}$ no phase transition can be induced in free flow at the bottleneck.

We have found that the minimum capacity C_{min} can depend considerably on the value q_{on}. In particular, at other model parameters than those used in Fig. 8 we can also find that $C_{min} > q_{out}$.

In contrast with the minimum capacity C_{min}, the threshold flow rate q_{out} does not depend on q_{on} [104]. This is because the minimum capacity C_{min} is associated with an S→F transition caused by the overacceleration effect introduced in three-phase traffic theory (Sec. I) [101]. In contrast, q_{out} is associated with an F→J transition caused by the overdeceleration effect of the GM model class.

We have found that the maximum capacity C_{max} of the KKSW CA model is always smaller than the critical flow rate $q_{cr}^{(B)}$ for spontaneous F→J transition of the NaSch CA model (Fig. 8):

$$C_{max} < q_{cr}^{(B)}. \tag{38}$$

Thus the critical flow rate $q_{cr}^{(B)}$ for spontaneous F→J transition cannot be reached in the three-phase theory. This is because, as shown above, in the three-phase theory at any flow rate q_{sum} at which either an F→J transition or F→S transition is possible, the probability of the F→S transition at the bottleneck is considerably larger than that for the F→J transition.

The metastability of free flow with respect to the F→J transition caused by the traffic-flow instability of the GM model class can be represented in the flow-density plane by a well-known line J that intersects the curve for free flow in the threshold point q_{out} [Fig. 10(a)]. However, this well-known theoretical result discovered in 1994 [42], which is the theoretical basis of a huge number of further theoretical studies of traffic flow (see references in [7,8,16,44]), has no relation to the metastability of free flow observed in real measured traffic data. This metastability of free flow simulated with the KKSW CA model can be represented in the flow-density plane by the minimum capacity C_{min} and the maximum capacity C_{max} of free flow (F) together with synchronized flow points related to the flow rate and density within synchronized flow at the bottleneck [Fig. 10(b)].

B. About macroscopic and microscopic definitions of synchronized flow and wide-moving jam traffic phases

Synchronized flow (S) is defined as congested traffic whose downstream front is fixed at a bottleneck. In contrast, rather than being fixed at the bottleneck, the downstream front of a wide-moving jam (J) propagates upstream while maintaining the mean velocity of the downstream front of the jam [14].

These phase definitions are *macroscopic* ones. However, in Figs. 5(b), 5(c), and 5(e), "dark lines" at the bottleneck are seen. Therefore one might have an assumption that the downstream front of congested traffic consisting of sequences of wide-moving jams is also fixed at the bottleneck. This assumption would contradict the macroscopic definition of the phase S. To resolve this problem, we consider microscopic (single-vehicle) features of congested traffic just upstream of the on-ramp bottleneck. To distinguish the traffic phases in microscopic data of congested traffic, we should consider a *microscopic* criterion of a wide-moving jam that is as follows [105–109]:

$$\frac{\tau_{\max}}{\tau_{\mathrm{del,\ J}}^{(\mathrm{acc})}} \gg 1. \tag{39}$$

In (39), $\tau_{\max}$ is the maximum time headway between two vehicles following each other within the jam, and $\tau_{\mathrm{del,\ J}}^{(\mathrm{acc})}$ is given by formula (32). Condition (39) determines the existence of a flow interruption interval in congested traffic. As shown in [105] and Sec. 2.6 of [15], *microscopic* definitions of the phases J and S, which are based on condition (39), are adequate to the macroscopic phase definitions.

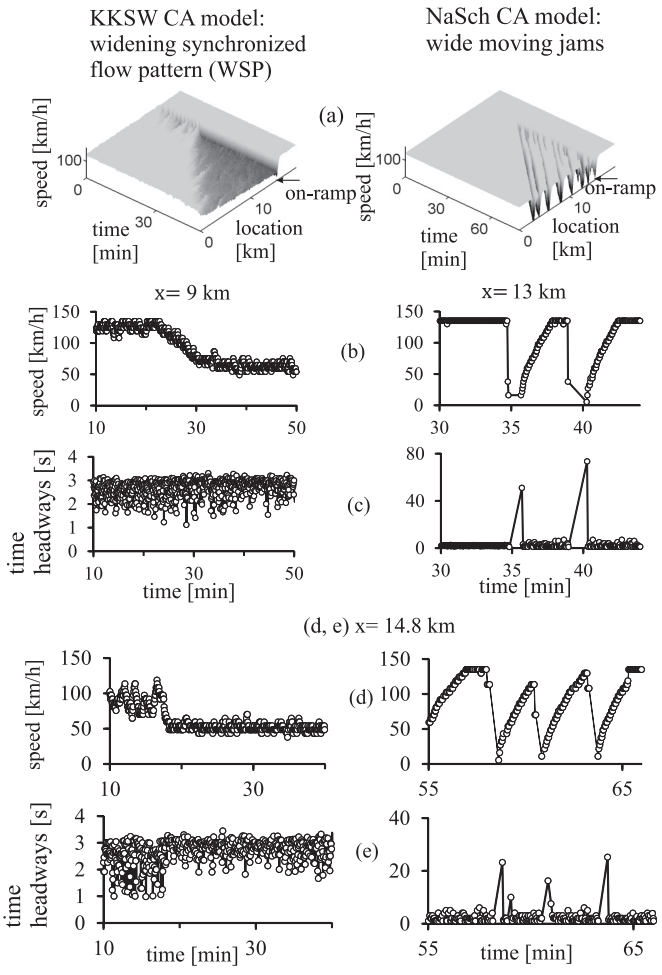

FIG. 11. Microscopic features of widening synchronized flow pattern (WSP) in the KKSW CA model (left panel) and wide-moving jams in the NaSch CA model (right panel) at on-ramp bottleneck. (a) Speed in time and space for WSP related to Fig. 4(a) (left) and for wide-moving jams related to Fig. 5(b) (right). (b–e) Single vehicle speed (b, d) and time headways (c, e) of vehicles measured at different road locations 9 km (b, c, left), 13 km (b, c, right), and 14.8 km (200 m upstream of the bottleneck) (d, e).

In particular, microscopic characteristics of an WSP resulting from the breakdown [Figs. 11(b) and 11(c), left panel] show that the microscopic criterion for the jam (39) is not satisfied, i.e., the WSP belongs indeed to the phase S.

In contrast, as can be seen from Fig. 11(c), right, the microscopic criterion (39) is satisfied for the moving jams shown in Fig. 11(a), right. The microscopic criterion (39) is also satisfied for these moving jams at road location $x =$ 14.8 km [Fig. 11(e), right]. This road location is 200 m upstream of the beginning of the on-ramp that is at $x = 15$ km.

Therefore, in contrast with above-made assumption about the reason for "dark lines" at the bottleneck in Figs. 5(b), 5(c), and 5(e), the sequence of these jams belongs to the phase J. Indeed, we see that there is *free flow* between the formation of moving jams at $x = 14.8$ km [Fig. 11(d), right]. This means that the downstream front of congested traffic consisting of sequences of wide-moving jams shown in Figs. 5(b), 5(c), and 5(e) is *not* fixed at the bottleneck.

In contrast with the sequence of wide-moving jams [Figs. 11(d) and 11(e), right], for the WSP [Figs. 11(d) and 11(e), left] neither criterion (39) is satisfied nor there is free flow at location $x = 14.8$ km. Therefore the downstream front of the WSP is fixed at the bottleneck, as required in the macroscopic definition of the phase S.

"Dark lines" at the bottleneck seen in Figs. 5(b), 5(c), and 5(e) are associated with a local speed decrease occurring when vehicles merge from the on-ramp lane to the main road. This speed disturbance always appears in free flow within the merging region of the on-ramp bottleneck that in the model is between locations $15 \leqslant x \leqslant 15.3$ km. However, in the CA models, there are nonrealistic large model speed fluctuations. These model fluctuations lead also to a nonrealistic large speed disturbance within the on-ramp merging region $15 \leqslant x \leqslant 15.3$ km. As shown in [89], the nonrealistic large speed disturbance influences none of the qualitative results of the analysis of phase transitions in traffic flow.

VI. CONCLUSIONS

At given flow rates at the bottleneck, to induce an F→J transition in a metastable free flow at the bottleneck through the application of a time-limited on-ramp inflow impulse, in both the KKSW and NaSch CA models, *the same critical amplitude* of the impulse is required.

If a smaller on-ramp inflow impulse than this critical one is applied, neither F→J transition nor other phase transitions can occur in the NaSch CA model: free flow recovers at the bottleneck. In contrast with the NaSch CA model, in the KKSW CA model, if the same smaller impulse is applied, then an F→S transition can be induced at the bottleneck.

In other words, at given flow rates at the bottleneck either the F→J transition or the F→S transition is possible in the KKSW CA model. However, the F→S transition occurs through a *considerably smaller* critical disturbance in the free flow than that required for the F→J transition. This explains why rather

than the F→J transition, in the three-phase theory traffic breakdown at a highway bottleneck is governed by the F→S transition in a metastable free flow, as observed in real measured traffic data.

In both the three-phase and two-phase traffic-flow theories, the threshold flow rate for the F→J transition, at which a moving jam can still be induced, is equal to the flow rate in free flow occurring in the outflow from a wide-moving jam q_{out}.

In the three-phase traffic theory, the threshold flow rate for induced F→S transition determines a minimum highway capacity $C_{\min}$. If the flow rate is smaller than $C_{\min}$, no traffic breakdown is possible.

The minimum capacity $C_{\min}$ of the three-phase theory has a qualitatively different physical sense as that of the outflow rate q_{out} from a wide-moving jam that determines the threshold flow rate for the F→J transition. For this reason, depending on model parameters, $C_{\min}$ can be either smaller or larger than q_{out}. When $C_{\min} < q_{\text{out}}$, there is a range of the flow rate downstream of the bottleneck within which traffic breakdown is possible to occur; however, no moving jams can persist in traffic flow.

The explanation of traffic breakdown at a highway bottleneck by an F→S transition in a metastable free flow at the bottleneck is the basic assumption of three-phase theory [1,2,14]. Traffic flow models of the GM model class cannot show the F→S transition. As shown in [16], induced traffic breakdown at the bottleneck (empirical feature 2 of traffic breakdown of Sec. I) is not possible in the framework of the LWR theory; this is because there is no free flow metastability in the LWR theory.

On the one hand, neither traffic-flow models of the GM model class nor traffic-flow models in the framework of the LWR theory incorporate a possibility of an F→S transition in a metastable free flow at the bottleneck introduced in the three-phase theory. Therefore, in accordance with the classical theory by Kuhn [110], the three-phase theory is *incommensurable* with all other traffic-flow theories. On the other hand, empirical traffic breakdown in real traffic flow is an F→S transition in a metastable free flow at the bottleneck. For this reason, both traffic-flow models of the GM model class and traffic-flow models in the framework of the LWR theory fail in the explanation of the set of fundamental features of traffic breakdown.

ACKNOWLEDGMENTS

We thank the German Federal Ministry of Economics and Technology for support through the project "UR:BAN - Urban Space: User oriented assistance systems and network management."

[1] B. S. Kerner, in *Proceedings of the 3rd Symposium on Highway Capacity and Level of Service*, edited by R. Rysgaard (Road Directorate, Ministry of Transport, Denmark, 1998), Vol. 2, pp. 621–642; Phys. Rev. Lett. **81**, 3797 (1998); B. S. Kerner, in *Traffic and Granular Flow' 97*, edited by M. Schreckenberg and D. E. Wolf (Springer, Singapore, 1998), pp. 239–267.

[2] B. S. Kerner, Transp. Res. Rec. **1678**, 160 (1999); B. S. Kerner, in *Transportation and Traffic Theory*, edited by A. Ceder (Elsevier Science, Amsterdam, 1999), pp. 147–171; Physics World **12**, 25–30 (1999).

[3] C. F. Daganzo, M. J. Cassidy, and R. L. Bertini, Transp. Res. A **33**, 365 (1999).

[4] M. Schönhof and D. Helbing, Transp. Sci. **41**, 135 (2007).

[5] M. Schönhof and D. Helbing, Transp. Res. B **43**, 784 (2009).

[6] M. Treiber, A. Kesting, and D. Helbing, Transp. Res. B **44**, 983 (2010).

[7] D. Helbing, Rev. Mod. Phys. **73**, 1067 (2001).

[8] M. Treiber and A. Kesting, *Traffic Flow Dynamics* (Springer, Berlin, 2013).

[9] B. S. Kerner and S. L. Klenov, J. Phys. A: Math. Gen. **35**, L31 (2002).

[10] B. S. Kerner, S. L. Klenov, and D. E. Wolf, J. Phys. A: Math. Gen. **35**, 9971 (2002).

[11] B. S. Kerner and S. L. Klenov, Phys. Rev. E **68**, 036130 (2003).

[12] B. S. Kerner, in *Encyclopedia of Complexity and System Science*, edited by R. A. Meyers (Springer, Berlin, 2009), pp. 9302–9355; 9355–9411; B. S. Kerner and S. L. Klenov, in *Encyclopedia of Complexity and System Science*, edited by R. A. Meyers (Springer, Berlin, 2009), pp. 9282–9302.

[13] B. S. Kerner and S. L. Klenov, Phys. Rev. E **80**, 056101 (2009).

[14] B. S. Kerner, *The Physics of Traffic* (Springer, Berlin, New York, 2004).

[15] B. S. Kerner, *Introduction to Modern Traffic Flow Theory and Control* (Springer, Berlin, New York, 2009).

[16] B. S. Kerner, Physica A **392**, 5261 (2013).

[17] A. D. May, *Traffic Flow Fundamentals* (Prentice-Hall, Inc., Englewood Cliffs, NJ, 1990).

[18] *Highway Capacity Manual* 2000 (National Research Council, Transportation Research Board, Washington, DC, 2000).

[19] *Highway Capacity Manual* 2010 (National Research Council, Transportation Research Board, Washington, DC, 2010).

[20] F. L. Hall and K. Agyemang-Duah, Transp. Res. Rec. **1320**, 91 (1991).

[21] F. L. Hall, V. F. Hurdle, and J. H. Banks, Transp. Res. Rec. **1365**, 12 (1992).

[22] L. Elefteriadou, R. P. Roess, and W. R. McShane, Transp. Res. Rec. **1484**, 80 (1995).

[23] B. N. Persaud, S. Yagar, and R. Brownlee, Transp. Res. Rec. **1634**, 64 (1998).

[24] M. Lorenz and L. Elefteriadou, Transp. Res. Circular **E-C018**, 84 (2000).

[25] W. Brilon, M. Regler, and J. Geistefeld, Straßenverkehrstechnik, Heft **3**, 136 (2005).

[26] W. Brilon and H. Zurlinden, Straßenverkehrstechnik, Heft **4**, 164 (2004).

[27] W. Brilon, J. Geistefeldt, and M. Regler, *Traffic and Transportation Theory*, edited by H. S. Mahmassani (Elsevier Science, Amsterdam, 2005), pp. 125–144.

[28] J. Geistefeldt and W. Brilon, in *Transportation and Traffic Theory 2009*, edited by W. H. K. Lam, S. C. Wong, and H. K. Lo, (Springer, New York, 2009), pp. 583–602.

[29] L. Elefteriadou, *An Introduction to Traffic Flow Theory, Springer Optimization and Its Applications*, Vol. 84 (Springer, Berlin, 2014).

[30] B. S. Kerner, Physica A **397**, 76 (2014).

[31] B. S. Kerner, H. Rehborn, R.-P. Schäfer, S. L. Klenov, J. Palmer, S. Lorkowski, and N. Witte, Physica A **392**, 221 (2013).

[32] C. W. Gardiner, *Handbook of Stochastic Methods*, 2nd ed. (Springer, Berlin, 1990).

[33] M. J. Lighthill and G. B. Whitham, Proc. Roy. Soc. A **229**, 281 (1955).

[34] P. I. Richards, Oper. Res. **4**, 42 (1956).

[35] C. F. Daganzo, Transp. Res. B **28**, 269 (1994).

[36] C. F. Daganzo, Transp. Res. B **29**, 79 (1995).

[37] R. Herman, E. W. Montroll, R. B. Potts, and R. W. Rothery, Oper. Res. **7**, 86 (1959).

[38] D. C. Gazis, R. Herman, and R. B. Potts, Oper. Res. **7**, 499 (1959).

[39] D. C. Gazis, R. Herman, and R. W. Rothery, Oper. Res. **9**, 545 (1961).

[40] *Traffic Flow Theory*, edited by N. H. Gartner, C. J. Messer, and A. Rathi (Transportation Research Board, Washington, DC, 2001); D. C. Gazis, *Traffic Theory* (Springer, Berlin, 2002).

[41] B. S. Kerner and P. Konhäuser, Phys. Rev. E **48**, R2335(R) (1993).

[42] B. S. Kerner and P. Konhäuser, Phys. Rev. E **50**, 54 (1994).

[43] B. S. Kerner, P. Konhäuser, and M. Schilke, Phys. Rev. E **51**, 6243 (1995).

[44] D. Chowdhury, L. Santen, and A. Schadschneider, Phys. Rep. **329**, 199 (2000); T. Nagatani, Rep. Prog. Phys. **65**, 1331 (2002); K. Nagel, P. Wagner, and R. Woesler, Oper. Res. **51**, 681 (2003); R. Mahnke, J. Kaupužs, and I. Lubashevsky, Phys. Rep. **408**, 1 (2005).

[45] As mentioned in Sec. I, in three-phase theory the overacceleration effect determines a traffic-flow instability that causes a growing wave of local *increase* in vehicle speed from an initial synchronized flow speed to a free flow speed (S→F transition). However, this instability can occur only if a traffic-flow model can show the synchronized flow traffic phase (S), including metastable states with respect to an S→F transition [Fig. 1(c)] [2, 14, 15]. It should be emphasized that two-phase traffic-flow models, in particular, that are described by ordinary differential equations, including GM class models [39, 40, 44], can show overacceleration due to a time delay in vehicle acceleration. However, the two-phase traffic models *cannot* describe the synchronized flow phase. For this reason, two-phase traffic-flow models cannot describe the S→F and F→S phase transitions.

[46] B. S. Kerner and S. L. Klenov, J. Phys. A: Math. Gen. **37**, 8753 (2004).

[47] B. S. Kerner, Phys. Rev. E **85**, 036110 (2012).

[48] B. S. Kerner, S. L. Klenov, G. Hermanns, and M. Schreckenberg, Physica A **392**, 4083 (2013).

[49] L. C. Davis, Phys. Rev. E **69**, 016108 (2004).

[50] H. K. Lee, R. Barlović, M. Schreckenberg, and D. Kim, Phys. Rev. Lett. **92**, 238702 (2004).

[51] R. Jiang and Q.-S. Wu, J. Phys. A: Math. Gen. **37**, 8197 (2004).

[52] K. Gao, R. Jiang, S.-X. Hu, B.-H. Wang, and Q.-S. Wu, Phys. Rev. E **76**, 026105 (2007).

[53] L. C. Davis, Physica A **368**, 541 (2006).

[54] L. C. Davis, Physica A **361**, 606 (2006).

[55] L. C. Davis, Physica A **387**, 6395 (2008).

[56] L. C. Davis, Physica A **388**, 4459 (2009).

[57] L. C. Davis, Physica A **389**, 3588 (2010).

[58] L. C. Davis, Physica A **391**, 1679 (2012).

[59] R. Jiang, M.-B. Hua, R. Wang, and Q.-S. Wu, Phys. Lett. A **365**, 6 (2007).

[60] R. Jiang and Q.-S. Wu, Phys. Rev. E **72**, 067103 (2005).

[61] R. Jiang and Q.-S. Wu, Physica A **377**, 633 (2007).

[62] R. Wang, R. Jiang, Q.-S. Wu, and M. Liu, Physica A **378**, 475 (2007).

[63] A. Pottmeier, C. Thiemann, A. Schadschneider, and M. Schreckenberg, in *Traffic and Granular Flow'05*, edited by A. Schadschneider, T. Pöschel, R. Kühne, M. Schreckenberg, and D. E. Wolf (Springer, Berlin, 2007), pp. 503–508.

[64] X. G. Li, Z. Y. Gao, K. P. Li, and X. M. Zhao, Phys. Rev. E **76**, 016110 (2007).

[65] J. J. Wu, H. J. Sun, and Z. Y. Gao, Phys. Rev. E **78**, 036103 (2008).

[66] J. A. Laval, in *Traffic and Granular Flow'05*, edited by A. Schadschneider, T. Pöschel, R. Kühne, M. Schreckenberg, and D. E. Wolf (Springer, Berlin, 2007), pp. 521–526.

[67] S. Hoogendoorn, H. van Lint, and V. L. Knoop, Transp. Res. Rec. **2088**, 102 (2008).

[68] B. S. Kerner, J. Phys. A: Math. Theor. **41**, 215101 (2008).

[69] K. Gao, R. Jiang, B.-H. Wang, and Q.-S. Wu, Physica A **388**, 3233 (2009).

[70] B. Jia, X.-G. Li, T. Chen, R. Jiang, and Z.-Y. Gao, Transportmetrica **7**, 127 (2011).

[71] J.-F. Tian, B. Jia, X.-G. Li, R. Jiang, X.-M. Zhao, and Z.-Y. Gao, Physica A **388**, 4827 (2009).

[72] S. He, W. Guan, and L. Song, Physica A **389**, 825 (2009).

[73] C.-J. Jin, W. Wang, R. Jiang, and K. Gao, J. Stat. Mech. (2010) P03018.

[74] S. L. Klenov, in *Proceedings of the Moscow Institute of Physics and Technology* (Moscow Institute of Physics and Technology (State University), Moscow, 2010), Vol. 2, no. 4, pp. 75–90, in Russian.

[75] A. V. Gasnikov, S. L. Klenov, E. A. Nurminski, Y. A. Kholodov, and N. B. Shamray, *Introduction to Mathematical Simulations of Traffic Flow* (MCNMO, Moscow, 2013), in Russian.

[76] S. Kokubo, J. Tanimoto, and A. Hagishima, Physica A **390**, 561 (2011).

[77] H.-K. Lee and B.-J. Kim, Physica A **390**, 4555 (2011).

[78] C.-J. Jin and W. Wang, Physica A **390**, 4184 (2011).

[79] J. P. L. Neto, M. L. Lyra, and C. R. da Silva, Physica A **390**, 3558 (2011).

[80] P. Zhang, C.-X. Wu, and S. C. Wong, Physica A **391**, 456 (2012).

[81] W.-H. Lee, S.-S. Tseng, J.-L. Shieh, and H.-H. Chen, IEEE Trans. ITS **12**, 1047 (2011).

[82] S. Lee, B. Heydecker, Y. H. Kim, and E.-Y. Shon, J. Adv. Transp. **4**, 143 (2011).

[83] J.-F. Tian, Z.-Z. Yuana, M. Treiber, B. Jia, and W.-Y. Zhanga, Physica A **391**, 3129 (2012).

[84] M. Kimathi, Ph.D. Thesis, Technische Universität Kaiserslautern, 2012; https://kluedo.ub.uni-kl.de/frontdoor/index/index/docId/2899.

[85] R. Borsche, M. Kimathi, and A. Klar, Comp. Math. Appl. **64**, 2939 (2012).

[86] Y. Wang, Y. I. Zhang, J. Hu, and L. Li, Int. J. Mod. Phys. C **23**, 1250060 (2012).

[87] J.-f. Tian, Z.-z. Yuan, B. Jia, H.-q. Fan, and T. Wang, Phys. Lett. A **376**, 2781 (2012).

[88] Y. Qiu, J. Non-Newtonian Fluid Mech. **197**, 1 (2013).

[89] B. S. Kerner, S. L. Klenov, and M. Schreckenberg, Phys. Rev. E **84**, 046110 (2011).

[90] H. Yang, J. Lu, X. Hu, and J. Jiang, Physica A **392**, 4009 (2013).

[91] F. Knorr and M. Schreckenberg, J. Stat. Mech. (2013) P07002.

[92] Xiang Zheng-Tao, Li Yu-Jin, Chen Yu-Feng, and Xiong Li, Physica A **392**, 5399 (2013).

[93] A. R. Mendez and R. M. Velasco, J. Phys. A: Math. Theor. **46**, 462001 (2013).

[94] Rui Jiang, Mao-Bin Hu, H. M. Zhang, Zi-You Gao, Bin-Jia, Qing-Song Wu, Bing Wang, and Ming Yang, PLOS One **9**, e94351 (2014).

[95] B. S. Kerner and S. L. Klenov, J. Phys. A: Math. Gen. **39**, 1775 (2006).

[96] B. S. Kerner, Europhys. Lett. **102**, 28010 (2013).

[97] K. Nagel and M. Schreckenberg, J. Phys. (France) I **2**, 2221 (1992).

[98] R. Barlović, L. Santen, A. Schadschneider, and M. Schreckenberg, Eur. Phys. J. B **5**, 793 (1998).

[99] A. Schadschneider, D. Chowdhury, and K. Nishinari, *Stochastic Transport in Complex Systems* (Elsevier Science, New York, 2011).

[100] In accordance with known results [10, 89], we have found that traffic breakdown can also be induced at the bottleneck through the upstream propagation of a localized congested pattern, which has earlier occurred downstream of the bottleneck.

[101] Simulations show that the closer the value of the flow rate q_{sum} to the minimum capacity C_{min}, the shorter the mean lifetime T_{life} of a synchronized flow pattern (SP) resulting from the breakdown. This is because a random return S→F transition can easily occur at the bottleneck due to model fluctuations at small enough values $q_{\text{sum}} - C_{\text{min}}$ [Fig. 3(d)]. Thus the value of minimum capacity C_{min} is determined by a stochastic process of spontaneous dissolution of a congested pattern that emerges after traffic breakdown at the bottleneck. A consideration of such a stochastic process is out of scope of this article. For simplicity, by an approximate calculation of the minimum capacity C_{min} [Figs. 3(a) and 3(b)], we consider the value $q_{\text{sum}} = C_{\text{min}}$ at which an SP exists on average about 10 min after it has been induced at the bottleneck.

[102] To find the probability of spontaneous traffic breakdown $P^{(\text{B})}$, a study of traffic breakdown at the bottleneck during the time interval T_{ob} is repeated for N different realizations (runs) for the same set of flow rates q_{in} and q_{on}. Different realizations are related to different initial conditions (at $t = 0$) chosen for random model fluctuations in the KKSW CA model (1)–(16). At the chosen on-ramp inflow rate, at any flow rate q_{in} at which spontaneous breakdown occurs, a widening synchronized flow pattern (WSP) emerges at the bottleneck [Figs. 4(a) and 4(b)]. Under condition $q_{\text{sum}} \geqslant C_{\text{max}}$, during the chosen time interval T_{ob} traffic breakdown occurs with the probability $P^{(\text{B})}(q_{\text{sum}}) = 1$. We have found that the larger the difference $q_{\text{sum}} - C_{\text{max}}$, the shorter the time interval T_{ob} at which spontaneous traffic breakdown occurs with the probability $P^{(\text{B})}(q_{\text{sum}}) = 1$ and the shorter the mean value of breakdown time delay $T^{(\text{B})}$.

[103] Under a chosen on-ramp inflow rate of $q_{\text{on}} = 400$ vehicles/h and other model parameters, either a spontaneous or induced F→S transition results in the emergence of synchronized flow patterns (SP) at the bottleneck [Figs. 3(c)–3(f) and 4(a), 4(b), and 4(d)]. However, in accordance with well-known results [10, 48], we have found that when q_{on} increases, then after the F→S transition has occurred at the bottleneck, wide-moving jams emerge later spontaneously in synchronized flow (S→J transition); as a result, rather than an SP, a general pattern (GP) occurs at the bottleneck. A study of GPs is out of the scope of this article.

[104] The jam outflow rate q_{out} [Figs. 2(a) and 2(c)] as the threshold for the F→J transition in a metastable free flow has first been found by Kerner and Konhäuser in a study of wide-moving jams [42] in a version of Payne's macroscopic model [107, 108] that belongs to the GM model class. A generalization of this result for arbitrary values of the on-ramp inflow rate q_{on} made by Helbing *et al.* [7, 8, 109] is given by the equation $q_{\text{on}} + q_{\text{in}} = q_{\text{out}}$. This equation determines a boundary for induced pattern formation in the diagram of congested patterns at the bottleneck for two-phase traffic-flow models of the GM model class derived by Helbing *et al.* [7, 8, 109].

[105] B. S. Kerner, S. L. Klenov, and A. Hiller, J. Phys. A: Math. Gen. **39**, 2001 (2006); Nonlinear. Dyn. **49**, 525 (2007); B. S. Kerner, S. L. Klenov, A. Hiller, and H. Rehborn, Phys. Rev. E **73**, 046107 (2006).

[106] See simulations of this instability in Figs. 18 and 19 of [48]. A more detailed consideration of features of the growing wave of a local speed increase caused by the instability due to the overacceleration effect is out of scope of this article.

[107] H. J. Payne, in *Mathematical Models of Public Systems*, edited by G. A. Bekey (Simulation Council, La Jolla, CA, 1971), Vol. 1, pp. 51–60.

[108] H. J. Payne, Transp. Res. Rec. **772**, 68 (1979).

[109] D. Helbing, A. Hennecke, and M. Treiber, Phys. Rev. Lett. **82**, 4360 (1999).

[110] T. S. Kuhn, *The Structure of Scientific Revolutions*, 4th ed. (The University of Chicago Press, Chicago, IL, 2012).